Mem. S.A.It. Vol. 82, 133

Memorie della

Radiative signatures of Fermi acceleration at relativistic shocks

B. Reville and J. G. Kirk

Max-Planck-Institut für Kernphysik, Saupfercheckweg 1, D-69117 Heidelberg, Germany
e-mail: brian.reville@mpi-hd.mpg.de

Abstract. The first-order Fermi process at relativistic shocks requires the generation of strong turbulence in the vicinity of the shock front. Recent particle in cell simulations have demonstrated that this mechanism can be studied self-consistently at weakly magnetised shocks. The radiative signature of this first-order Fermi acceleration mechanism is important for models of both the prompt and afterglow emission in gamma-ray bursts and depends on the strength parameter $a = \lambda e|\delta B|/mc^2$ of the fluctuations (λ is the length-scale and $|\delta B|$ the magnitude of the fluctuations.) For electrons (and positrons), acceleration saturates when the radiative losses produced by the scattering cannot be compensated by the energy gained on crossing the shock. For Weibel mediated shocks, this sets an upper limit on the energy of the photons radiated during the scattering process: $\hbar\omega_{\rm max} < 40\,{\rm Max}(a,1)\left(n/1\,{\rm cm}^{-3}\right)^{1/6}\bar{\gamma}^{-1/6}\,{\rm eV}$, where n is the number density of the plasma and $\bar{\gamma}$ the thermal Lorentz factor of the downstream plasma, provided $a < a_{\rm crit} \sim 10^6$. For shocks mediated by the synchrotron maser instability, this upper limit can be considerably higher, although this depends on the strength of the magnetic field, which has a large uncertainty.

Key words. radiation mechanisms: non-thermal — acceleration of particles — gamma rays: bursts

1. Introduction

Particle acceleration at relativistic shocks is thought to proceed via the first order Fermi acceleration mechanism (see Kirk & Duffy 1999, and references therein). Recent particle in cell (PIC) simulations have demonstrated that the process can indeed occur, under favourable conditions (Spitkovsky 2008; Martins et al. 2009; Sironi & Spitkovsky 2009). These simulations are *ab initio* in the sense that the process is reproduced from Maxwell's equations and the equations of motion.

The maximum achievable particle energy can be determined by several factors, including the shock's lifetime or its spatial extent. Ultimately, the acceleration ceases when the radiative energy losses that are inevitably associated with the scattering process overwhelm the energy gains obtained upon crossing the shock.

Such effects are usually not included in PIC simulations because of the difficulties associated with radiation reaction. However, for a given model of pitch angle diffusion, it is possible to derive an approximate upper limit for the maximum particle energy. Exactly when

Send offprint requests to: B. Reville

this happens will depend on the details of the scattering process. Current simulations suggest small angle scattering is a necessary condition for Fermi acceleration to occur. The presence of a large scale field generally acts to suppress the acceleration as particle are effectively transported into the far downstream region (Sironi & Spitkovsky 2009).

2. Particle transport and acceleration

For the purpose of estimating radiative signatures of accelerated particles, it is convenient to characterise the fluctuations in terms of their 'strength' parameter a, defined as the ratio of their length scale to the length defined by typical fluctuations in the field strength: $a = \lambda e|\delta B|/mc^2$ (e.g Landau & Lifshitz 1975). According to this strength parameter, the transport can be divided into two distinct regimes, which we call 'ballistic' ($a < \gamma$) and 'helical' ($a > \gamma$). In ballistic transport, the scattering mean free path is shorter than the gyroradius in the local field. On the other hand, in the helical transport regime, gyro motion is only slightly perturbed. Particles have sufficient time to gyrate about the field while their pitch angles and guiding-centre positions diffuse.

Ballistic transport regime:

At a relativistic shock, a particle remains in the upstream medium until it has been deflected, on average, through an angle of $1/\bar{\gamma}$ in the upstream rest frame. In the downstream the particle must deflect through a much larger angle $\sim \pi/2$. A turbulent fluctuation of strength parameter a, deflects a particle of Lorentz factor γ through an angle a/γ. Provided this angle is small, the diffusion coefficient is simply $\mathcal{D}_\theta = a^2\nu_{\rm sc}/\gamma^2$, where $\nu_{\rm sc}$ is the mean scattering frequency. The average number of scatterings in the upstream medium between shock encounters is therefore $N_{\rm scatt,u} \approx (\gamma/a_{\rm u}\bar{\gamma})^2$, and likewise in the downstream $N_{\rm scatt,d} \approx (\gamma/a_{\rm d})^2$.

Assuming similar size strength parameters either side of the shock, radiative losses in the downstream dominate. For kinematic reasons, the average energy gain per cycle is roughly a factor of two (Achterberg et al. 2001), so that the acceleration process will saturate when the energy lost in the upstream medium is roughly γmc^2. This implies that in the absence of inverse Compton cooling, the energy is limited to (Kirk & Reville 2010)

$$\gamma < \left(\frac{3mc^2\lambda_{\rm d}}{2e^2}\right)^{1/3} \qquad (1)$$

Helical transport regime:

In the helical transport regime, energy losses are important at all points along a trajectory. In the Bohm limit, the maximum Lorentz factor is (Achterberg et al. 2001):

$$\gamma < \left(\frac{3m^2c^3}{2e^3B}\right)^{1/2} \qquad (2)$$

At magnetised, relativistic shocks, particle acceleration by the first-order Fermi mechanism is less plausible, since it relies on strong cross-field diffusion. However, if the process does operate, particles can move from the helical to the ballistic regime, as their Lorentz factor increases. There exists a critical strength parameter $a_{\rm crit}$ such that when $a = a_{\rm crit}$ the maximum Lorentz factor $\gamma_{\rm max}$ is achieved just at the point at which the transport changes character from helical to ballistic, i.e.

$$a_{\rm crit} = \left(\frac{3mc^2\lambda_{\rm d}}{2e^2}\right)^{1/3} \qquad (3)$$

If $a > a_{\rm crit}$, all particles remain in the the helical regime. On the other hand, if $a < a_{\rm crit}$, particles of the maximum Lorentz factor undergo ballistic transport, but lower energy particles may be in the helical regime.

Combining the constraints from the ballistic regime (1) and the helical regime (2) gives:

$$\gamma_{\rm max} = \begin{cases} a_{\rm crit} & \text{for } a < a_{\rm crit} \\ a_{\rm crit}\sqrt{a_{\rm crit}/a} & \text{for } a > a_{\rm crit} \end{cases} \qquad (4)$$

3. Radiative signatures

To estimate the maximum photon energy that can be produced by the highest energy particles, we consider the radiation emitted when a particle is scattered by a single fluctuation of strength parameter a. The character of the

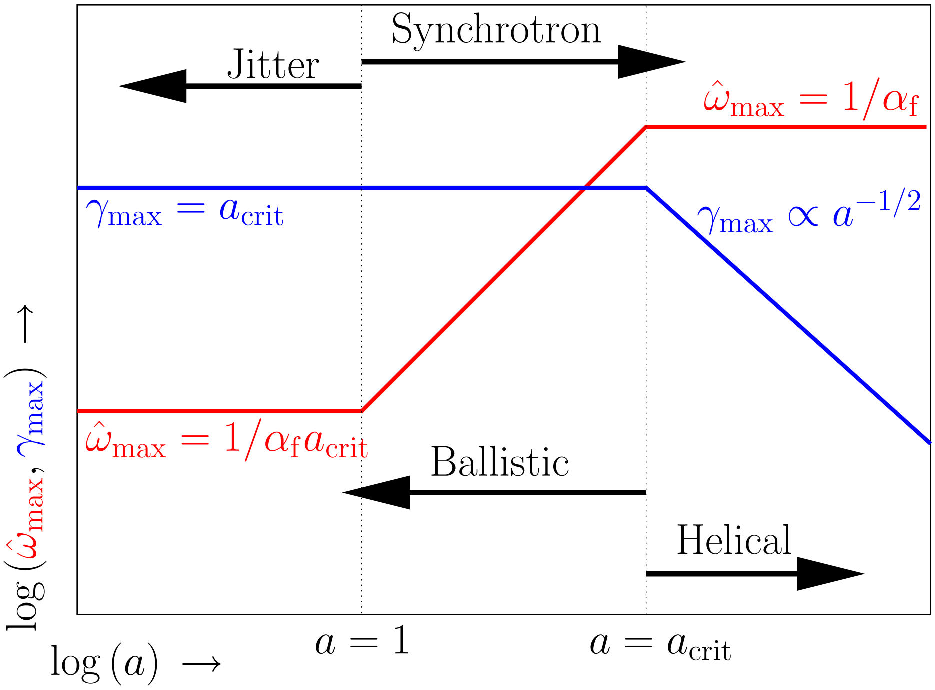

Fig. 1. The maximum electron Lorentz factor $\gamma_{\rm max}$ and the maximum photon energy $\hat{\omega}_{\rm max} = \hbar\omega_{\rm max}/mc^2$ radiated when scattered by magnetic fluctuations of strength a at a relativistic shock. The jitter/synchrotron regimes are separated by the vertical $a = 1$ line; the ballistic/helical transport regimes by the $a = a_{\rm crit}$ line.

emission depends crucially on the "formation" or "coherence" length of the radiated photons. If $a > 1$, the formation length is roughly $\lambda_{\rm coh} \approx mc^2/eB$. This is much smaller than the wavelength of the turbulence, so that the individual photons are created in regions in which the field is almost constant and homogeneous. The result is synchrotron radiation, with the emissivity defined by the local value of the field. The emission extends up to the roll-over frequency of the highest energy electrons:

$$\omega_{\rm max} \approx 0.5a\gamma^2 c/\lambda \qquad \text{for } a > 1 \tag{5}$$

If, on the other hand, $a < 1$, the particle is deflected through an angle that is small compared to $1/\gamma$. In this case, the coherence length is no longer limited by deflection, but is given by the distance moved by the particle in the lab. frame during the time it takes for the photon to move one wavelength ahead of the particle: $\lambda_{\rm coh} \approx \gamma^2 c/\omega$. The maximum frequency is roughly

$$\omega_{\rm max} \approx 0.5\gamma_{\rm max}^2 c/\lambda \qquad \text{for } a < 1 \tag{6}$$

In each case, most of the power radiated by an individual electron emerges within a decade of the roll-over frequency that corresponds to its Lorentz factor. Therefore, the spectrum radiated by a power-law distribution of electrons, with differential number density $dn/d\gamma \propto \gamma^{-p}$, for both the synchrotron and jitter cases, reproduces the standard power-law spectrum at frequencies between the roll-over frequency of the highest and lowest energy electrons: $dL/d\omega \propto \omega^{-(p-1)/2}$.

Combining the limit on the Lorentz factor (1) with the expressions for the roll-over frequency (5) and (6), one finds for the maximum frequency that can be radiated by particles accelerated at a relativistic shock front:

$$\frac{\hbar\omega_{\rm max}}{mc^2} = \begin{cases} (\alpha_{\rm f} a_{\rm crit})^{-1} & a < 1 \\ a\,(\alpha_{\rm f} a_{\rm crit})^{-1} & 1 < a < a_{\rm crit} \\ \alpha_{\rm f}^{-1} & a > a_{\rm crit} \end{cases} \quad (7)$$

where $\alpha_{\rm f} = e^2/\hbar c$ is the fine structure constant. The results are summarised in Fig. 1.

4. Discussion

As mentioned in the introduction, PIC simulations exhibiting Fermi acceleration require the presence of small scale turbulence. For sufficiently weakly magnetised shocks, the field is generated via the Weibel instability. These typically have magnetic structures of size on the order of the plasma skin-depth $\lambda = \ell_{\rm w} c/\omega_{\rm p}$ where $\omega_{\rm p}$ is the local plasma frequency, and $\ell_{\rm w} \sim 10$.

For magnetised shocks mediated by the synchrotron maser instability, the characteristic length in the downstream plasma $\lambda_{\rm s,d}$ is dictated by the requirement that the incoming particles be significantly deflected, giving $\lambda_{\rm s} = \ell_{\rm s}\bar{\gamma} mc^2/eB_{\rm d}$ with $\ell_{\rm s} \sim 1$ (Lyubarsky 2006).

It follows that for a given shock, the critical strength parameter is

$$a_{\rm crit} \approx \begin{cases} 10^6 \ell_{\rm w}^{1/3} \bar{\gamma}^{1/6} \left(n/1\,{\rm cm}^3\right)^{-1/6} & \text{Weib} \\ 10^4 \ell_{\rm s}^{1/3} \bar{\gamma}^{1/3} \left(B/1\,{\rm mG}\right)^{-1/3} & \text{Synch} \end{cases} \quad (8)$$

While these results are derived assuming a electron-positron plasma, the dependence on mass is weak, and for an electron-ion shock, $a_{\rm crit}$ increases by less than an order of magnitude.

Current PIC simulations suggest strength parameters $\sim \bar{\gamma}$ (Sironi & Spitkovsky 2009). This suggests a maximum photon energy of $\sim \Gamma\bar{\gamma}/\alpha_{\rm f} a_{\rm crit}$, where Γ is the Lorentz factor of the downstream flow in the observer's frame (neglecting the host galaxy's redshift), which can be as large as 10^3. For Weibel mediated shocks, this sets an upper limit of

$$\hbar\omega_{\rm max} \lesssim 40 \left(\frac{n}{1\,{\rm cm}^{-3}}\right)^{1/6} \left(\frac{\Gamma}{10^3}\right) \bar{\gamma}^{5/6}\,{\rm keV}, \quad (9)$$

which cannot account for the gamma-ray production in the prompt phase. This of course does not exclude the possibility of Compton scattering of the soft jitter or synchrotron photons to produce gamma-rays.

For shocks mediated by the synchrotron maser instability, the limit is not so severe

$$\hbar\omega_{\rm max} \lesssim \left(\frac{B}{1\,{\rm mG}}\right)^{1/3} \left(\frac{\Gamma}{10^3}\right) \bar{\gamma}^{2/3}\,{\rm MeV}, \quad (10)$$

where we have adopted a magnetic field strength of 1 mG. The actual value of the magnetic field in the internal shocks of a GRB can in principle be several orders of magnitude larger. If magnetic field values on the order of kilo-Gauss can be generated in the vicinity of the internal shocks, it may be possible to produce GeV photons at a synchrotron maser instability mediated shock.

Acknowledgements. BR gratefully acknowledges support from the Alexander von Humboldt foundation.

References

Achterberg, A., Gallant, Y. A., Kirk, J. G., & Guthmann, A. W. (2001), MNRAS, 328, 393

Kirk, J. G., & Duffy, P. 1999, Journal of Physics G Nuclear Physics, 25, 163

Kirk, J. G., & Reville, B., 2010, ApJL, 710, L16

Landau, L. D., & Lifshitz, E. M. 1975, The classical theory of fields (Oxford: Pergamon Press, 1975)

Lyubarsky, Y. 2006, ApJ, 652, 1297

Martins, S. F., Fonseca, R. A., Silva, L. O., & Mori, W. B. 2009, ApJl, 695, L189

Sironi, L., & Spitkovsky, A. 2009, ApJ, 698, 1523

Spitkovsky, A. 2008, ApJL, 682, L5